

# Evaluation of +S2 sea ice forecast and some other better title

Elio Campitelli<sup>1,2</sup>, Ariaan Purich<sup>1,2</sup>, Julie Arblaster<sup>1,2</sup>, Eun-Pa Lim<sup>3</sup>, Matthew Wheeler<sup>3</sup>, and Phillip Reid<sup>3</sup>

<sup>1</sup>School of Earth, Atmosphere and Environment, Monash University, Australia

<sup>2</sup>Securing Antarctica's Environmental Future, Monash University, Australia

<sup>3</sup>Bureau of Meteorology

**Correspondence:** Elio Campitelli (elio.campitelli@monash.edu)

**Abstract.** The abstract goes here. It can also be on *multiple lines*.

. The author's copyright for this publication is transferred to institution/company.

## 1 Introduction

Unlike Arctic sea ice, which has been steadily retreating at least since the start of satellite records in the early 80s,  
5 Antarctic sea ice has experienced a slightly increasing trend that models systematically failed to reproduce and puzzled researchers ([Hobbs et al.](#)). Then, in 2016 Antarctic sea ice extent dropped precipitously and has been at low and record low levels since, highlighting even more our lack of understanding of Antarctic sea ice variability and change ([Espinosa et al.](#)).

Antarctic sea ice is in a remote location but the potential impacts of its variability extends far into the lower latitudes,  
10 affecting the circulation of both the ocean and the atmosphere, ocean carbon uptake and biological processes. It's likely that a reduction in sea ice extent would reduce the meridional temperature gradient which in turn would reduce the strength and location of the eddy-driven jet (and vice versa for an increase in sea ice), which is a crucial component of weather events. In the northern hemisphere, it has been hypothesised that the reduction in Arctic sea ice has lead to a weaker, wavier jet, increasing the frequency of extreme events ([Barnes and Screen](#)). There is some evidence of  
15 this effect in the Southern Hemisphere. Models show a weakened vortex in the middle atmosphere, increased vertical wave flux and greater zonal wave 1 amplitude in Springs following a low sea ice maximum. But models don't fully agree on the exact phase of the zonal wave response and observations don't show a clear signal ([Rea et al.](#)). The jet response to sea ice loss is also very model dependent, particularly sensitive to its the climatological location and relatively small compared with the direct effect of CO<sub>2</sub> increase and Sea Surface Temperature (SST) warming ([Ayres and Screen](#)). On climate scales, it is thought that the temperature signal of a reduction in Antarctic sea ice mirrors a

“mini global warming” and experiments also predict a weakening and northerly shift of the eddy-driven (Raphael et al.; England et al., a, b; Ayres et al.).

Correctly modelling Antarctic sea ice is not only necessary for process understanding and climate projections to inform adaptation strategies. Accurate seasonal to subseasonal forecast are crucial for operations in and around the Antarctic continent such as scientific missions, fisheries and tourism (De Silva et al., Wagner et al.). However, producing accurate Antarctic sea ice forecasts has been challenging due to model biases and inherent large variability and complexity and it has lagged behind Arctic sea ice forecasts (Zampieri et al.). Dynamical seasonal forecasts of summer Antarctic sea ice have been shown to perform worse than relatively simple statistical methods (Massonnet et al.), which also underscores the need for better understanding of sea ice dynamics.

In this work we evaluate sea ice forecasts produced by ACCESS-S2, the Australian Bureau of Meteorology subseasonal-to-seasonal prediction system. This evaluation will inform future work with the model as a research tool and explore the potential of using it as a sea ice forecasting tool.

## 2 Data and methods

### 2.1 ACCESS-S2

ACCESS-S2 (Wedd et al.) is the Australian Bureau of Meteorology current subseasonal-to-seasonal prediction system which replaced ACCESS-S1 (Hudson et al.) in October 2021. Both ACCESS-S2 and ACCESS-S1 consist on the Global Atmosphere 6.0 (GA6) (Williams et al.; Waters et al., a), Global Land 6.0 (Best et al.; Waters et al., a), Global Ocean 5.0 (Madec et al.; Megann et al.) and Global Sea Ice 6.0 [CICE; Rae et al.] model components. The atmosphere has a N216 horizontal resolution (~60km in the mid-latitudes) with 85 levels. The land model uses the same horizontal grid with 4 soil levels. The ocean component has a  $1/4^\circ$  resolution with 75 vertical levels. The ice component –based on CICE version 4.1– has the same resolution than the ocean and 5 sea ice categories as well as an open water category.

Both systems take atmospheric initial conditions derived from ERA-interim (Dee et al.) for the hindcast and from the Bureau’s operational analysis for real-time forecasts. The main difference between the two are the ocean and ice initial conditions. ACCESS-S1 initial conditions come from the Met Office FOAM system, which uses a multivariate, incremental three-dimensional variational (3D-Var), first-guess-at-appropriate-time (FGAT) data assimilation scheme (Waters et al., b) and assimilates sea surface temperature (SST), sea surface height (SSH), in situ temperature and salinity profiles, and sea ice concentration. ACCESS-S2, instead, runs from initial conditions generated by the in-house data assimilation scheme described in Wedd et al.. This scheme is a weakly coupled ensemble optimal interpolation method and assimilates temperature and salinity profiles from EN4 (Good et al.) for the hindcast and from the WMO Global Telecommunication System (GTS) and both the Coriolis and USGODAE Global Data

Assembly Centers (GDACs) for the real-time forecast. SSTs are nudged to Reynolds OISSTv2.1 (Reynolds et al.) for the hindcast and to the Global Australian Multi-Sensor SST Analysis (GAMSSA; Zhong and Beggs 2008) for the real-time forecast in areas where SSTs are over 0°C. Relevant for this work, sea ice concentrations are not assimilated.

55 The ACCESS-S2 hindcast used in this study runs for the period 1981–2018. Each forecast consists of 9 ensemble members, 3 of which run for 279 days and 6 for 42 days. Anomalies are taken with respect to the 1981–2011 climatology computed from the daily ACCESS-S2 reanalysis and smoothed with a 11 day running mean.

The ACCESS-S1 hindcast runs for the period 1990–2012, with 7-member forecasts integrated for 217 days. No reanalysis is available so we are not able to compute a climatology for this forecast, therefore we don't show metrics  
60 based on anomalies.

## 2.2 Verification datasets

For verification we use satellite-derived estimates of sea ice concentration, which estimates the proportion of each grid area that is covered with ice. Different datasets derived using different algorithms provide different estimates, each with its own biases and uncertainties. ? estimated that the inter-product uncertainty of sea ice extent is of the  
65 order of 1 million km<sup>2</sup>. As will be shown below, this spread is minimal compared with the errors in the ACCESS-S2 and ACCESS-S1 forecasts, so the conclusions are independent of the dataset used.

We use NOAA/NSIDC's Climate Data Record V4 [CDR; Meier et al. (b)] as the primary verification dataset. It takes the maximum value of the NASA Team (Cavalieri et al.) and NASA Bootstrap (Comiso) sea ice concentration products to reduce their low concentration bias (Meier et al., b, a). Both source algorithms use data from the  
70 Scanning Multichannel Microwave Radiometer (SMMR) on the Nimbus-7 satellite and from the Special Sensor Microwave/Imager (SSM/I) sensors on the Defense Meteorological Satellite Program's (DMSP) -F8, -F11, and -F13 satellites. The data has a resolution of 25 by 25km and daily from 1978 onwards.

The European Organisation for the Exploitation of Meteorological Satellites (EUMETSAT) Ocean and Sea Ice Satellite Application Facility (OSI SAF) (Facility) is another satellite-derived sea ice concentration product. It is  
75 based on mostly the same sensors as the NOA CDR but computed independently using different algorithms. Figures prepared with this dataset are provided in the supplementary material.

## 2.3 Error measures

For evaluation purposes, we use a series of measures.

Sea Ice Extent is defined as the area of ocean covered with at least 15% ice. This threshold is motivated by the  
80 limitations in satellite retrieval, which is increasingly unreliable for lower sea ice conditions.

Pan-Antarctic Sea Ice Extent serves as a rough global measure of the amount of sea ice but it doesn't take into account the spatial distribution. A model could have relatively accurate extent of ice but with different distributions. To account for location errors, we computed the Root Mean Squared Error (RMSE) of sea ice concentration anomalies and the Integrated Ice Edge Error [IIEE; [Goessling et al.](#)].

85 We compute RMSE as the square root of the average squared differences between forecasted and observed sea ice concentration anomalies. We compute a pan-Antarctic RMSE by averaging over the whole domain, and also a zonally-varying RMSE by averaging over 24 15° longitude slices around Antarctica.

The IIEE is defined as the area in which the model misspredicts sea ice concentration being above or below 15% ice. That is, dichotomise sea ice concentration into areas with more and less than 15% sea ice both in the forecast and  
90 observations; the IIEE is the area in which forecast and observations differ.

All error measures were computed on the NOAA/NSIDC CDRV4 domain grid and projection to which model output was bilinearly interpolated.

### 3 Results and discussion

#### 3.1 Reanalysis

95 3.1.1 Bias

Figure 1 a shows the seasonal cycle of Sea Ice Extent for the ACCESS-S2 hindcast and NOAA/NSIDC CDRV4 ACCESS-S2 shows a severe low extent bias, especially in the late summer-early autumn. This is due primarily to faster melt during a longer melt season between January and March and slower growth during March and April. This is then balanced with faster growth between May and July (Fig. 2). Many sea ice models exhibit this systematic  
100 underestimation during the sea ice minimum and early freezing season ([Massonnet et al.](#)) and could indicate problems in the representation of thermodynamics in the model ([Zampieri et al.](#)).

ACCESS-S1 has a smaller low bias than ACCESS-S2, especially at low lags (Fig. 1) even though the typical growth rates are very similar between both models (Fig. 2). At larger lags, ACCESS-S1's bias in summer and autumn is very similar to ACCESS-S2's. This suggests that this lower sea ice state is closer to the models' equilibrium, indicating  
105 that it is an issue with model formulation that was being corrected by the data assimilation system in ACCESS-S1 and not in ACCESS-S2.

At large lags, sea ice extent loses most of the initial condition memory and reverts to the model's preferred equilibrium state. Therefore we can estimate the latter using the hindcasts with the largest possible lag, which is shown in triangles in Figure 1 for the same dates as the initial conditions. The difference between the two is the effect of the  
110 data assimilation.

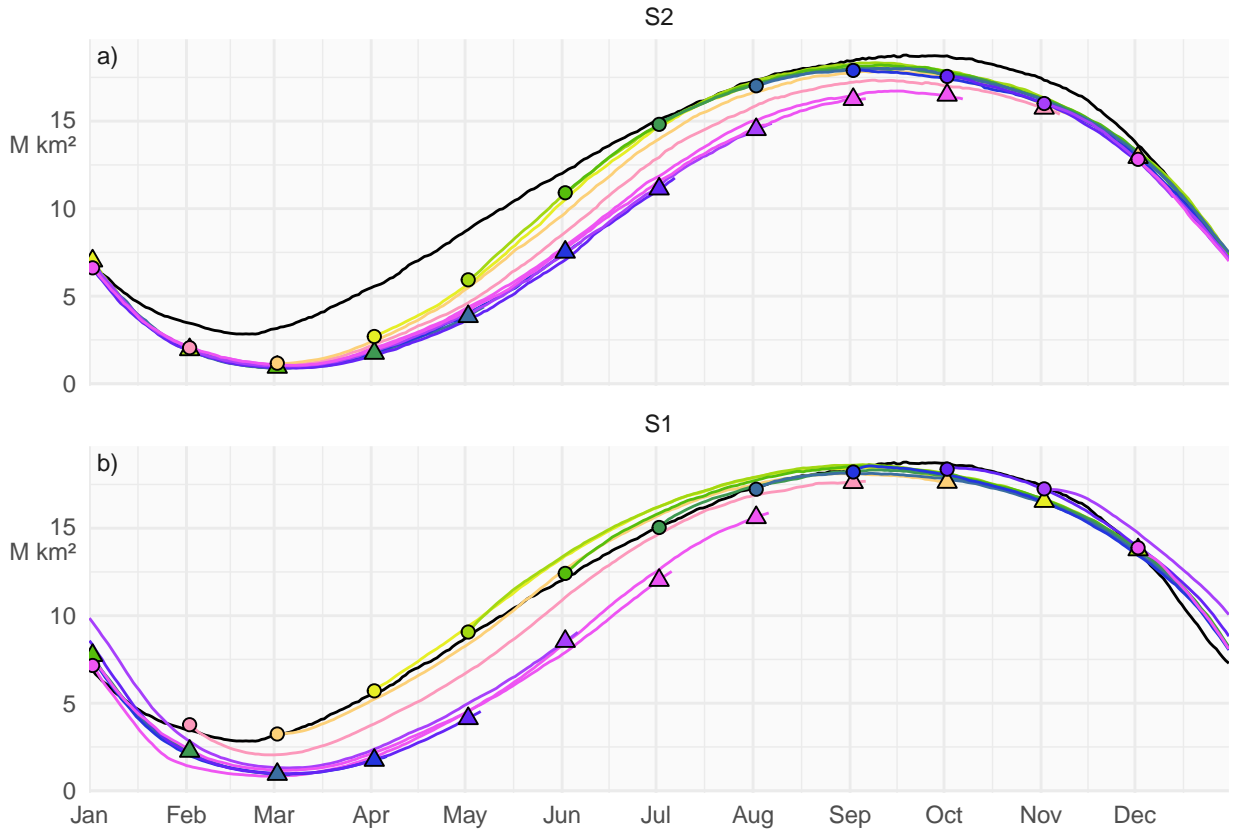


**Figure 1.** Median sea ice extent for all hindcasts initialised the first of the month for ACCESS-S2 and ACCESS-S1 in colours representing the start month. In black, the median sea ice extent of NOAA/NSIDC CDRV4.

The equilibrium of ACCESS-S1 and ACCESS-S2 is very similar (comparing the triangles in each panel in Fig. 1), owing to them having the same model formulation. From June to October, in ACCESS-S2 circles are closer to observations than to the triangles, indicating that the information from the ocean and atmosphere data assimilation is getting to sea ice and improving the initial conditions. The rest of the year, there is little if any difference between 115 circles and triangles in ACCESS-S2, indicating that almost no data assimilation is taking place and the sea ice component of the model is virtually free-running. In ACCESS-S1, on the other hand, circles are very close to observations year-round.

Figure 3 shows the difference of monthly mean sea ice concentrations between NOAA/NSIDC CDRV4 and ACCESS-S2 hindcasts at the shortest lag. From October to May, the model underestimates sea ice concentrations pretty much 120 everywhere there is ice except for the deep Weddell Sea in April and May, where sea ice concentrations saturate to 1 both in the observations and forecasts. In winter, the differences are mostly on the sea ice edge, with light positive

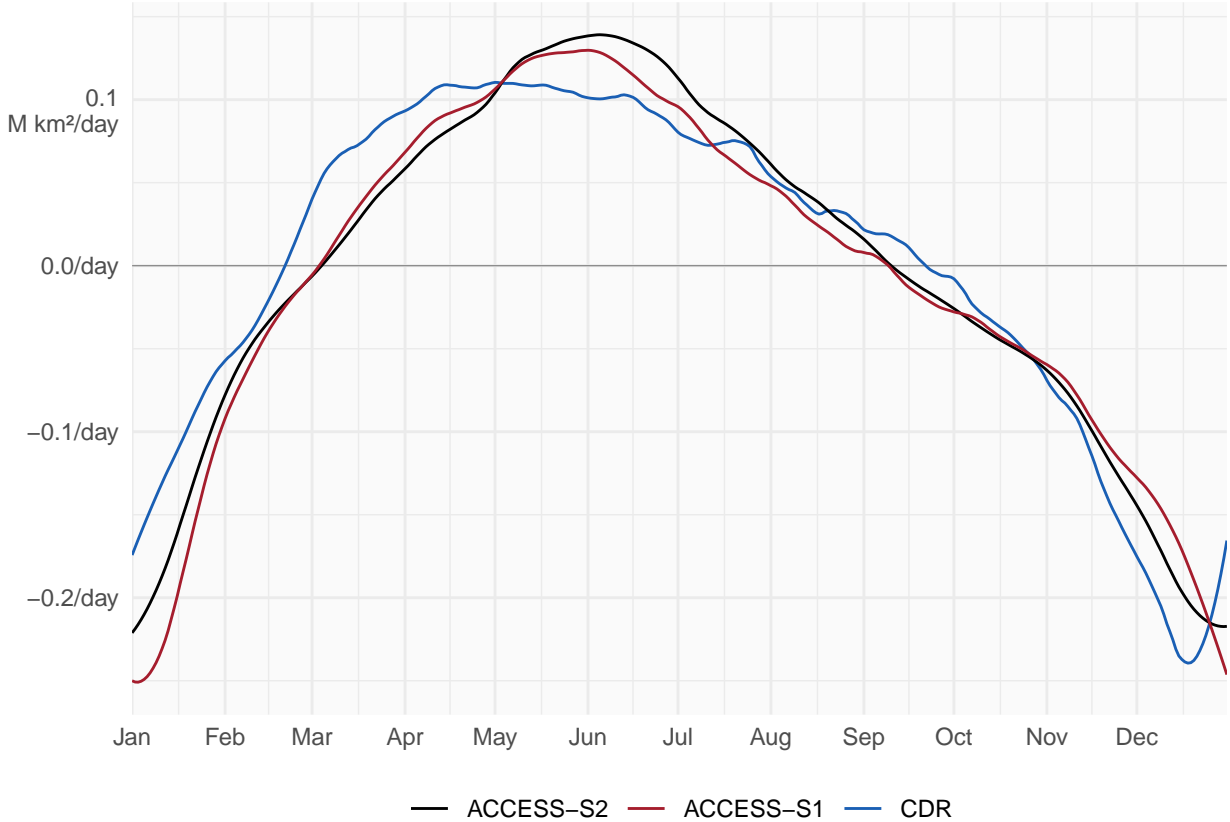


**Figure 2.** Median daily sea ice extent growth of ACCESS-S1 and ACCESS-S2 hindcasts and observations. Values are smoothed with a 2-degree loess smooth with a 30 day window.

bias in the African sector of East Antarctica and negative bias around the Indian Ocean sector which partially compensate, resulting in the near-zero extent bias seen in those months (Fig. 1).

### 3.1.2 Anomalies

125 Figure 4 shows monthly sea ice extent anomalies forecasted at selected lags. The anomalies in this case were computed with respect of the climatology of each lag, which works as a bias-correction method. Compared with ACCESS-S1, ACCESS-S2 anomaly forecast is relatively poor even in the first month, which stays relatively skilful even at lag 3. ACCESS-S2 shows much bigger variability than observations, with dramatic lows between 1995 and 2007 and highs between 2007 and 2015.

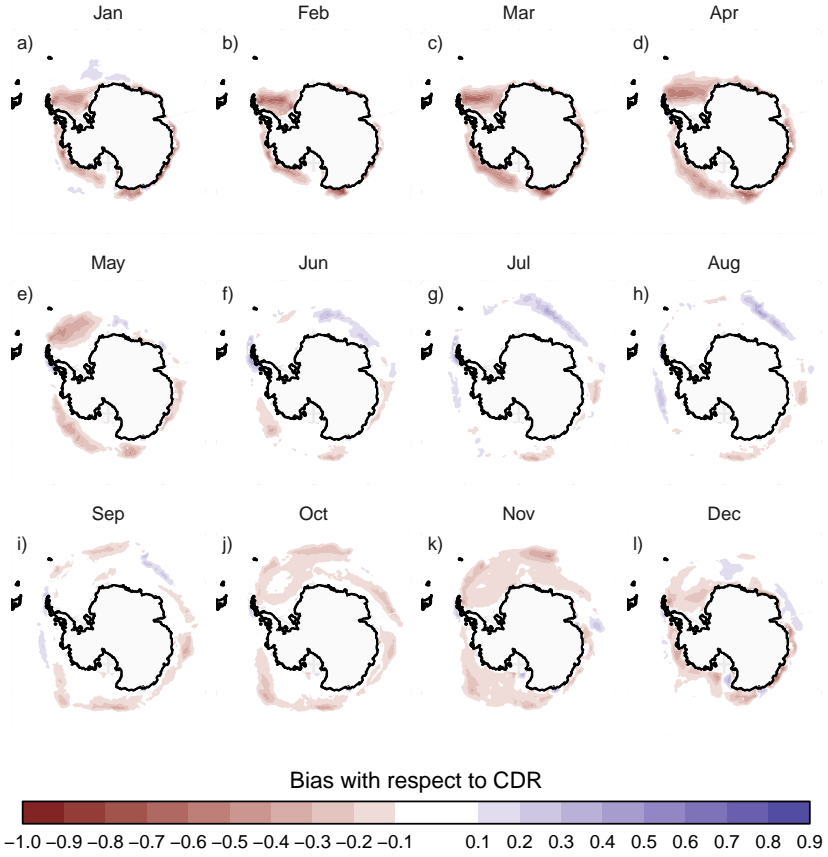
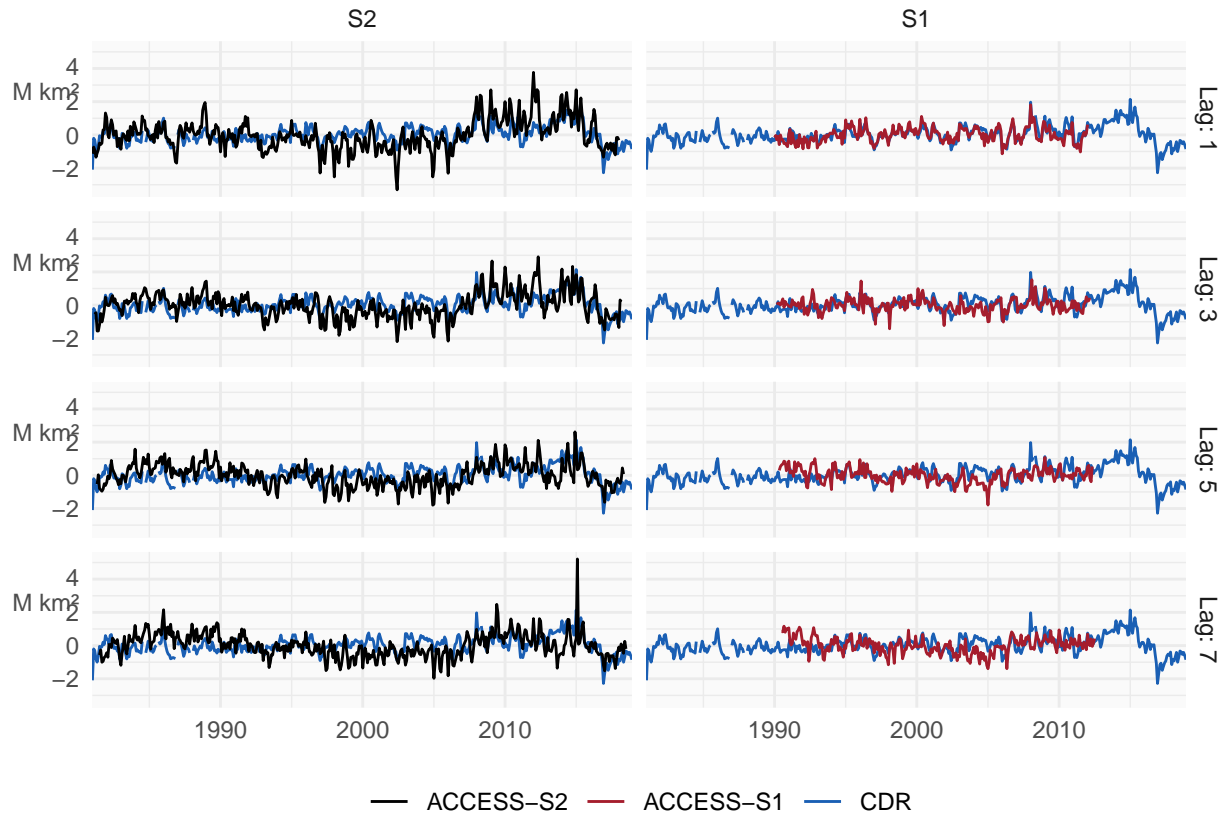


**Figure 3.** Mean sea ice concentrations 1-month lag monthly mean ACCESS-S2 forecast bias compared with NSIDC.

### 130 3.1.3 RMSE

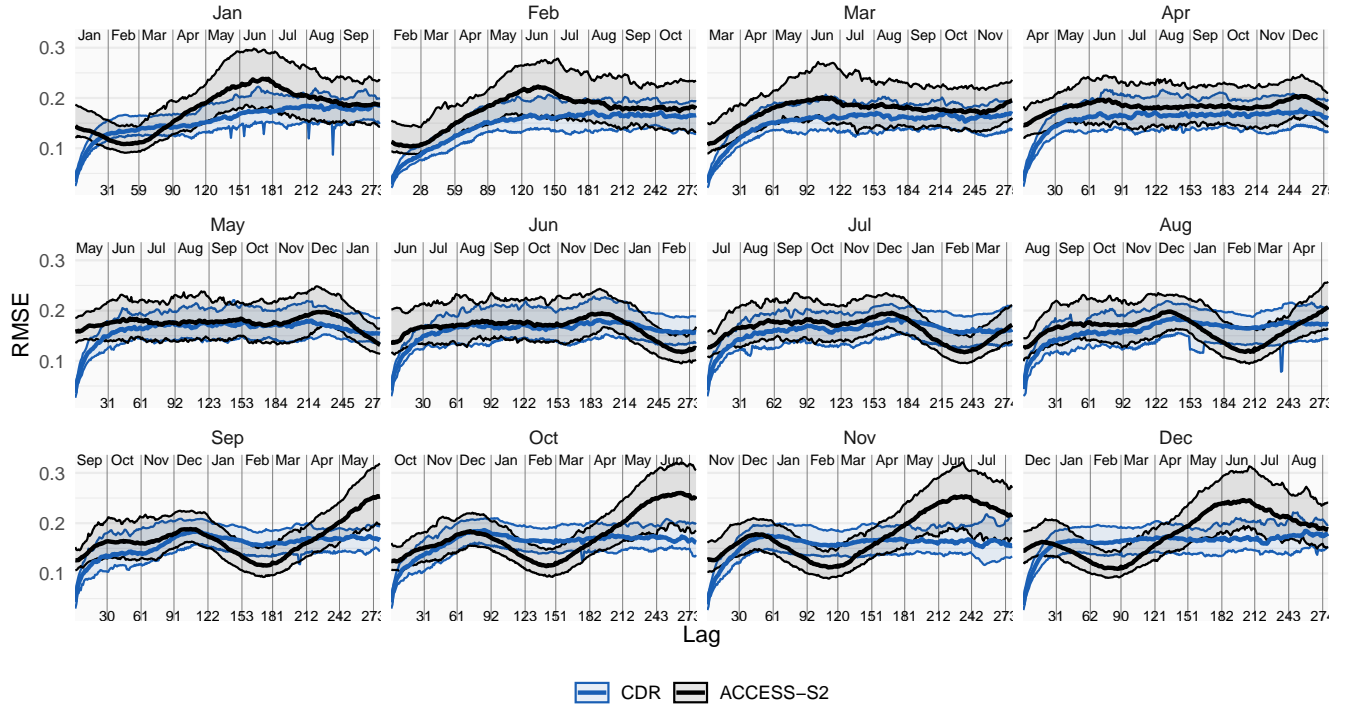
To study ACCESS-S2 forecasts quantitatively, we compute error measures for all hindcasts started on the 1st of every month.

Figure 5 shows the median and 95% range of RMSE of sea ice concentration anomalies for ACCESS-S2 forecasts compared with a benchmark of persistence. Due to errors in the initial conditions, it is expected that a persistence 135 forecast would be better than the model forecast at very short lags, but that the persistence forecast errors would grow faster and eventually surpass the mode forecast, after when it is statistically useful. Here the persistence errors are almost always lower than the ACCESS-S2 forecast, indicating that the model doesn't have skill at any lag and in any month. The only exception is around February, where the model has lower RMSE than the persistence forecast at virtually every lag.



**Figure 4.** Sea ice extent anomalies for ACCESS-S1 and ACCESS-S2 (black) and NOAA/NSIDC CDRV4 (blue).

- 140 Even though ACCESS-S2 is no better than persistence at forecasting pan-Antarctic sea ice concentration anomalies, the quality of the forecast might vary between regions. To analyse the spatial distribution of the model error, we computed sea ice concentration anomalies RMSE on 15 meridional slices  $24^\circ$  wide. The median difference between the forecast and persistence RMSE is shown on Figure 6, where negative values indicate that the model has lower RMSE than the benchmark.
- 145 The skill shown by ACCESS-S2 at February-March forecasts is evidenced by a band of negative values across almost all longitudes. The only region where February-March sea ice is not well forecasted is east of the Antarctic Peninsula, which is the only region with consistent summer sea ice. This suggests that the positive skill around the summer minimum comes from the model correctly forecasting no ice where no ice is ever found. However, there are other regions of skilful forecasts.
- 150 Forecasts initialised on January 1<sup>st</sup> (Fig. 6 panel a) show RMSE values below persistence at lags larger than 180 days (corresponding to July through September) in the Ross and Weddell Sea. These two regions are also relatively



**Figure 5.** Median and 95% coverage of sea ice concentration anomalies RMSE as a function of forecast lag for all forecast initialised on the first of each month compared with a reference forecast of persistence of anomalies.

well forecasted from other months. Notably, May forecasts of Weddell sea ice concentration anomalies (Fig. 6 panel e) are skilful after about 20 days and remain so until December. The Weddell Sea is also the region with the maximum error –around June regardless of initialisation date.

#### 155 3.1.4 Comparison with S1

To compare ACCESS-S2 with ACCESS-S1, we computed the IIEE for both models. This error measure is shown in Figure 7 for all lags and forecasts initialised at the first of every month. ACCESS-S1 has lower error at short lags at all months, with the errors converging to ACCESS-S2 as the forecast goes on. The time to convergence depends on the month and it can be as short as two weeks June and July to as long as 160 days for forecasts initialised in 160 February. Since the only difference between these forecasts are the initial conditions, this timescale is an indication of the the memory of sea ice to initial conditions –at least from October to March when the data assimilated form the other components has little to no influence on sea ice.

Also evident in Figure 7 is the difference in the error spread at short lags between ACCESS-S2 and ACCESS-S1. In all months ACCESS-S1 has much narrower error spread at lag 1. The error in the initial conditions is not only small,

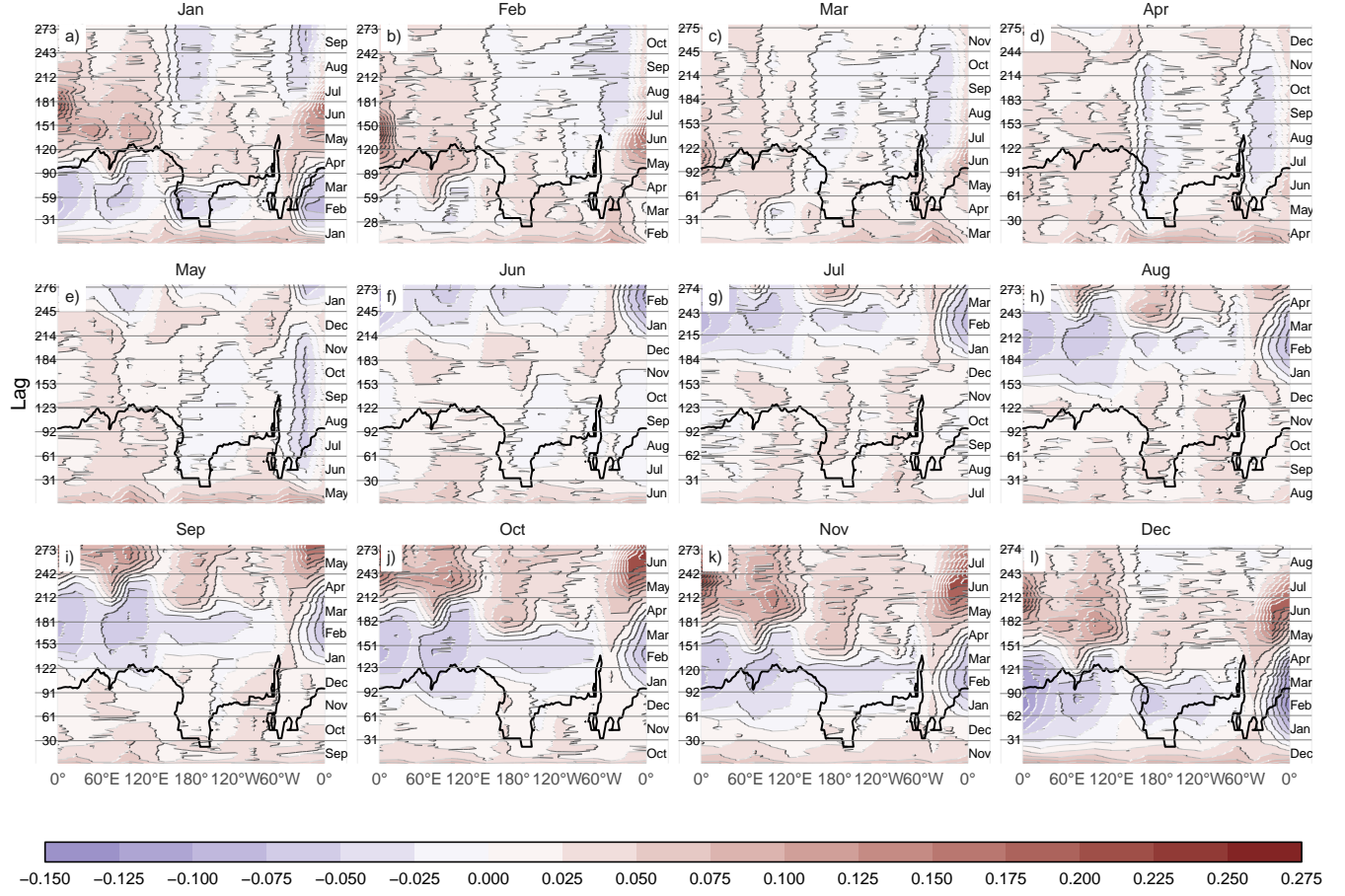


**Figure 6.** Meadian difference between RMSE of ACCESS-S2 forecasts and persistence forecast at longitudinal bands.

165 but also fairly constant. This spread then grows towards a climatological spread as errors accumulate differently in different forecasts. For ACCESS-S2, this is true only between July and October, approximately. For all other months, the error spread is more or less stable throughout the forecast window, indicating that not only the initial error is high, but it's not constant.

170 The large initial error spread could be due either to large spread of ensemble members or to large spread of individual forecasts. Figure 8 splits the IIEE variance for each lag into the mean variance of each individual forecast and the variance of the mean error of each individual forecast, which adds up to the total variance. The average variance of each forecast is almost identical between forecast systems in all months. This shows that the ensemble spread of individual forecasts evolves identically, which, again, it's not unexpected because both systems share the same model formulation. This also shows that the perturbation scheme in ACCESS-S2 is comparable to the one in ACCESS-S1.

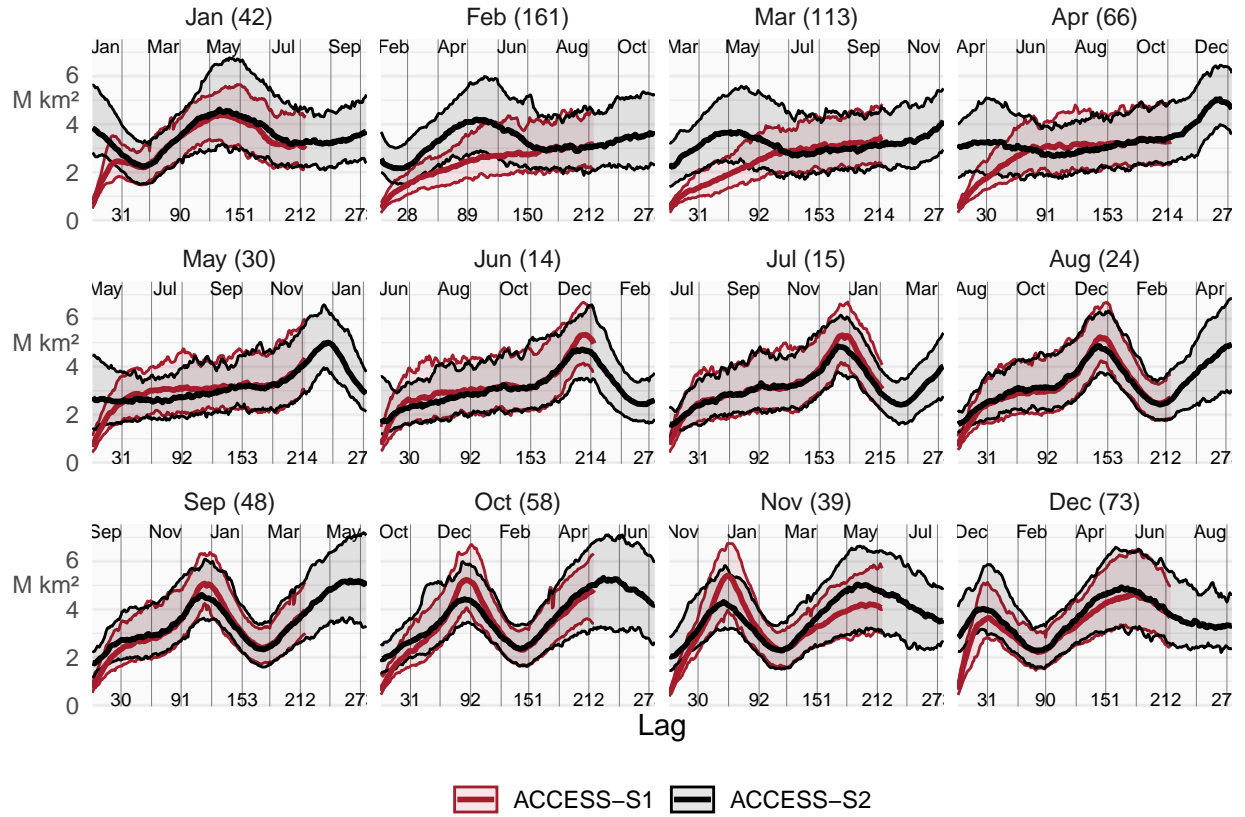


**Figure 7.** Median and 95% coverage of Integrated Ice Edge Error as a function of forecast lag for all forecasts initialised on the first of each month for ACCESS-S1 and ACCESS-S2 hindcasts. For each month, the number in parenthesis indicates the minimum lag at which the mean error of each model is not statistically significant at a 1% level using a two-sided t-test.

175 On the other hand, the spread of the mean error is always larger in ACCESS-S2 than ACCESS-S1. The difference is particularly large at short lags in some months, which coincide with the ones in which the data assimilation scheme is not influencing sea ice initial conditions.

### 3.2 Conclusions

Sea ice forecasts from the ACCESS-S2 model show a significant low extent bias, particularly during late summer 180 and early autumn. This bias is attributed to a faster and longer melt season between January and March, and slower growth between March and April. This underestimation during the minimum and early freezing season is a common issue in many seasonal-to-subseasonal (S2S) systems, suggesting potential problems either with the model's thermodynamic representation or with short wave radiation forcing, as shown in other climate models. Even though ACCESS-S2 shares the same model formulation with ACCESS-S1, the latter does not suffer from this bias. This is

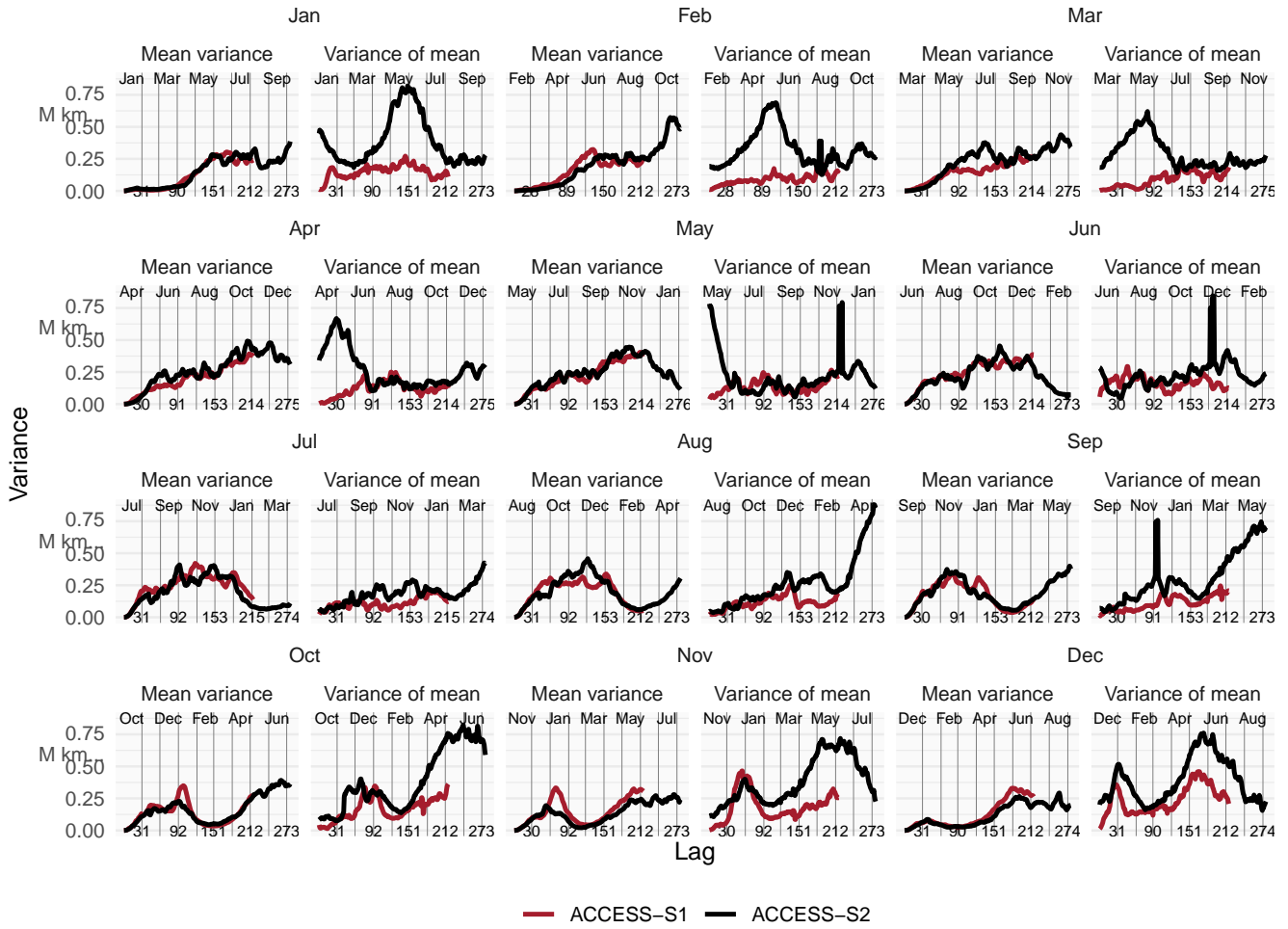


**Figure 8.** Mean spread of IIEE at different lags for different models.

185 due to the assimilation of sea ice concentration anomalies into the initial conditions, which successfully corrects for the negative bias in the model. The analysis suggests that the data assimilation system in ACCESS-S2 is only effectively influencing sea ice initial conditions from June to October, while the rest of the year, the sea ice component runs virtually free, reverting to its biased equilibrium state.

Analysis of the error spread shows that ACCESS-S2 initial conditions from December to May not only have large 190 errors, but that the initial error spread is very large compared with ACCESS-S1. This spread is not due to the perturbation scheme, since the mean error variance for individual forecasts is low and comparable with ACCESS-S1. Instead, it is due to large variance of the mean error of individual forecasts, which is comparable to the climatology

spread. This is further evidence that individual initial conditions are not being affected by the data assimilation scheme.

- 195 Based on the observation that ACCESS-S2 sea ice initial conditions are essentially not initialised, comparing its forecasts with ACCESS-S1's allows us to estimate the time-scale for which initial conditions are important. This highlights February initial conditions as a crucial for determining sea ice evolution at least up to late June. Arctic sea ice forecast also show greater sensitivity to initial conditions in (boreal) summer compared with (boreal) winter ([?Bunzel et al.](#)), so similar mechanism might be playing a role.
- 200 Although forecasts are not skilful for forecasting panantarctic sea ice concentrations, there are some areas where the model does show skill. The Weddell Sea, and the Ross Sea to a lesser extent are particularly well forecasted between June and November for forecasts initialised from January to June. These regions have been recognised as a regions of high predictability thanks to persistent and eastwardly advected upper ocean heat content anomalies ([Bushuk et al.](#)) Sea surface temperatures are assimilated by ACCESS-S2 only in areas with temperatures greater than 0°C
- 205 and errors don't show a clear easterly-propagating signal, so it is not clear if ACCESS-S2 is leveraging the same source of predictability.

---

#### 4 References

- Ayres, H. and Screen, J.: Multimodel Analysis of the Atmospheric Response to Antarctic Sea Ice Loss at Quadrupled CO<sub>2</sub>, 46, 9861–9869, <https://doi.org/10.1029/2019GL083653>.
- Ayres, H. C., Screen, J. A., Blockley, E. W., and Bracegirdle, T. J.: The Coupled Atmosphere–Ocean Response to Antarctic Sea Ice Loss, 35, 4665–4685, <https://doi.org/10.1175/JCLI-D-21-0918.1>.
- Barnes, E. A. and Screen, J. A.: The Impact of Arctic Warming on the Midlatitude Jet-Stream: Can It? Has It? Will It?, 6, 277–286, <https://doi.org/10.1002/wcc.337>.
- 210 Best, M. J., Pryor, M., Clark, D. B., Rooney, G. G., Essery, R. L. H., Ménard, C. B., Edwards, J. M., Hendry, M. A., Porson, A., Gedney, N., Mercado, L. M., Sitch, S., Blyth, E., Boucher, O., Cox, P. M., Grimmond, C. S. B., and Harding, R. J.: The Joint UK Land Environment Simulator (JULES), Model Description – Part 1: Energy and Water Fluxes, 4, 677–699, <https://doi.org/10.5194/gmd-4-677-2011>.
- Bunzel, F., Notz, D., Baehr, J., Müller, W. A., and Fröhlich, K.: Seasonal Climate Forecasts Significantly Affected by Observational Uncertainty of Arctic Sea Ice Concentration, 43, 852–859, <https://doi.org/10.1002/2015GL066928>.
- Bushuk, M., Winton, M., Haumann, F. A., Delworth, T., Lu, F., Zhang, Y., Jia, L., Zhang, L., Cooke, W., Harrison, M., Hurlin, B., Johnson, N. C., Kapnick, S. B., McHugh, C., Murakami, H., Rosati, A., Tseng, K.-C., Wittenberg, A. T., Yang, X., and Zeng, F.: Seasonal Prediction and Predictability of Regional Antarctic Sea Ice, 34, 6207–6233, <https://doi.org/10.1175/JCLI-D-20-0965.1>.
- 220 Cavalieri, D. J., Gloersen, P., and Campbell, W. J.: Determination of Sea Ice Parameters with the NIMBUS 7 SMMR, 89, 5355–5369, <https://doi.org/10.1029/JD089iD04p05355>.

- Comiso, J.: Bootstrap Sea Ice Concentrations from Nimbus-7 SMMR and DMSP SSM/I-SSMIS. (NSIDC-0079, Version 4)., <https://doi.org/10.5067/X5LG68MH013O>.
- De Silva, L. W. A., Inoue, J., Yamaguchi, H., and Terui, T.: Medium Range Sea Ice Prediction in Support of Japanese Research Vessel MIRAI's Expedition Cruise in 2018, 43, 223–239, <https://doi.org/10.1080/1088937X.2019.1707317>.
- 230 Dee, D. P., Uppala, S. M., Simmons, A. J., Berrisford, P., Poli, P., Kobayashi, S., Andrae, U., Balmaseda, M. A., Balsamo, G., Bauer, P., Bechtold, P., Beljaars, A. C. M., family=Berg, given=L., p. d. u., Bidlot, J., Bormann, N., Delsol, C., Dragani, R., Fuentes, M., Geer, A. J., Haimberger, L., Healy, S. B., Hersbach, H., Hölm, E. V., Isaksen, L., Källberg, P., Köhler, M., Matricardi, M., McNally, A. P., Monge-Sanz, B. M., Morcrette, J.-J., Park, B.-K., Peubey, C., family=Rosnay, given=P., p. u., Tavolato, C., Thépaut, J.-N., and Vitart, F.: The ERA-Interim Reanalysis: Configuration and Performance of the Data Assimilation System, 137, 553–597, <https://doi.org/10.1002/qj.828>.
- England, M., Polvani, L., and Sun, L.: Contrasting the Antarctic and Arctic Atmospheric Responses to Projected Sea Ice Loss in the Late Twenty-First Century, 31, 6353–6370, <https://doi.org/10.1175/JCLI-D-17-0666.1>, a.
- England, M. R., Polvani, L. M., Sun, L., and Deser, C.: Tropical Climate Responses to Projected Arctic and Antarctic Sea-Ice 240 Loss, 13, 275–281, <https://doi.org/10.1038/s41561-020-0546-9>, b.
- Espinosa, Z. I., Blanchard-Wrigglesworth, E., and Bitz, C. M.: Understanding the Drivers and Predictability of Record Low Antarctic Sea Ice in Austral Winter 2023, 5, 1–9, <https://doi.org/10.1038/s43247-024-01772-2>.
- Facility, E. O. a. S. I. S. A.: Global Sea Ice Concentration Climate Data Record 1978–2020 (v3.0, 2022), OSI-450-a.
- Goessling, H. F., Tietsche, S., Day, J. J., Hawkins, E., and Jung, T.: Predictability of the Arctic Sea Ice Edge, 43, 1642–1650, 245 <https://doi.org/10.1002/2015GL067232>.
- Good, S. A., Martin, M. J., and Rayner, N. A.: EN4: Quality Controlled Ocean Temperature and Salinity Profiles and Monthly Objective Analyses with Uncertainty Estimates, 118, 6704–6716, <https://doi.org/10.1002/2013JC009067>.
- Hobbs, W. R., Massom, R., Stammerjohn, S., Reid, P., Williams, G., and Meier, W.: A Review of Recent Changes in Southern Ocean Sea Ice, Their Drivers and Forcings, 143, 228–250, <https://doi.org/10.1016/j.gloplacha.2016.06.008>.
- 250 Hudson, D., Alves, O., Hendon, H. H., Lim, E.-P., Liu, G., Luo, J.-J., MacLachlan, C., Marshall, A. G., Shi, L., Wang, G., Wedd, R., Young, G., Zhao, M., and Zhou, X.: ACCESS-S1 The New Bureau of Meteorology Multi-Week to Seasonal Prediction System, 67, 132–159, <https://doi.org/10.1071/es17009>.
- Madec, G., Bourdallé-Badie, R., Bouttier, P.-A., Bricaud, C., Bruciaferri, D., Calvert, D., Chanut, J., Clementi, E., Coward, A., Delrosso, D., Ethé, C., Flavoni, S., Graham, T., Harle, J., Iovino, D., Lea, D., Lévy, C., Lovato, T., Martin, N., 255 Masson, S., Mocavero, S., Paul, J., Rousset, C., Storkey, D., Storto, A., and Vancoppenolle, M.: NEMO Ocean Engine, <https://doi.org/10.5281/zenodo.1475234>.
- Massonet, F., Barreira, S., Barthélémy, A., Bilbao, R., Blanchard-Wrigglesworth, E., Blockley, E., Bromwich, D. H., Bushuk, M., Dong, X., Goessling, H. F., Hobbs, W., Iovino, D., Lee, W.-S., Li, C., Meier, W. N., Merryfield, W. J., Moreno-Chamarro, E., Morioka, Y., Li, X., Niraula, B., Petty, A., Sanna, A., Scilingo, M., Shu, Q., Sigmond, M., Sun, N., Tietsche, S., Wu, X., Yang, Q., and Yuan, X.: SIPN South: Six Years of Coordinated Seasonal Antarctic Sea Ice Predictions, 10, 260 <https://doi.org/10.3389/fmars.2023.1148899>.
- Megann, A., Storkey, D., Aksenov, Y., Alderson, S., Calvert, D., Graham, T., Hyder, P., Siddorn, J., and Sinha, B.: GO5.0: The Joint NERC–Met Office NEMO Global Ocean Model for Use in Coupled and Forced Applications, 7, 1069–1092, <https://doi.org/10.5194/gmd-7-1069-2014>.

- 265 Meier, W. N., Fetterer, F., Windnagel, A. K., and Stewart, J. S.: NOAA/NSIDC Climate Data Record of Passive Microwave Sea Ice Concentration, <https://doi.org/10.7265/efmz-2t65>, a.
- Meier, W. N., Peng, G., Scott, D. J., and Savoie, M. H.: Verification of a New NOAA/NSIDC Passive Microwave Sea-Ice Concentration Climate Record, <https://doi.org/10.3402/polar.v33.21004>, b.
- Rae, J. G. L., Hewitt, H. T., Keen, A. B., Ridley, J. K., West, A. E., Harris, C. M., Hunke, E. C., and Walters, D. N.:  
270 Development of the Global Sea Ice 6.0 CICE Configuration for the Met Office Global Coupled Model, 8, 2221–2230, <https://doi.org/10.5194/gmd-8-2221-2015>.
- Raphael, M. N., Hobbs, W., and Wainer, I.: The Effect of Antarctic Sea Ice on the Southern Hemisphere Atmosphere during the Southern Summer, 36, 1403–1417, <https://doi.org/10.1007/s00382-010-0892-1>.
- Rea, D., Elsbury, D., Butler, A. H., Sun, L., Peings, Y., and Magnusdottir, G.: Interannual Influence of Antarctic Sea Ice on  
275 Southern Hemisphere Stratosphere-Troposphere Coupling, 51, e2023GL107478, <https://doi.org/10.1029/2023GL107478>.
- Reynolds, R. W., Smith, T. M., Liu, C., Chelton, D. B., Casey, K. S., and Schlax, M. G.: Daily High-Resolution-Blended Analyses for Sea Surface Temperature, 20, 5473–5496, <https://doi.org/10.1175/2007JCLI1824.1>.
- Wagner, P. M., Hughes, N., Bourbonnais, P., Stroeve, J., Rabenstein, L., Bhatt, U., Little, J., Wiggins, H., and Fleming, A.: Sea-Ice Information and Forecast Needs for Industry Maritime Stakeholders, 43, 160–187,  
280 <https://doi.org/10.1080/1088937X.2020.1766592>.
- Waters, J., Bell, M. J., Martin, M. J., and Lea, D. J.: Reducing Ocean Model Imbalances in the Equatorial Region Caused by Data Assimilation, 143, 195–208, <https://doi.org/10.1002/qj.2912>, a.
- Waters, J., Lea, D. J., Martin, M. J., Mirouze, I., Weaver, A., and While, J.: Implementing a Variational Data Assimilation System in an Operational 1/4 Degree Global Ocean Model, 141, 333–349, <https://doi.org/10.1002/qj.2388>, b.
- 285 Wedd, R., Alves, O., family=Burgh Day, given=Catherine, p. u., Down, C., Griffiths, M., Hendon, H. H., Hudson, D., Li, S., Lim, E.-P., Marshall, A. G., Shi, L., Smith, P., Smith, G., Spillman, C. M., Wang, G., Wheeler, M. C., Yan, H., Yin, Y., Young, G., Zhao, M., Xiao, Y., and Zhou, X.: ACCESS-S2: The Upgraded Bureau of Meteorology Multi-Week to Seasonal Prediction System, 72, 218–242, <https://doi.org/10.1071/ES22026>.
- Williams, K. D., Harris, C. M., Bodas-Salcedo, A., Camp, J., Comer, R. E., Copsey, D., Fereday, D., Graham, T., Hill, R.,  
290 Hinton, T., Hyder, P., Ineson, S., Masato, G., Milton, S. F., Roberts, M. J., Rowell, D. P., Sanchez, C., Shelly, A., Sinha, B., Walters, D. N., West, A., Woollings, T., and Xavier, P. K.: The Met Office Global Coupled Model 2.0 (GC2) Configuration, 8, 1509–1524, <https://doi.org/10.5194/gmd-8-1509-2015>.
- Zampieri, L., Goessling, H. F., and Jung, T.: Predictability of Antarctic Sea Ice Edge on Subseasonal Time Scales, 46, 9719–9727, <https://doi.org/10.1029/2019GL084096>.

295 **5 Supplementary figures**

. use this to add a statement when having data sets and software code available

. use this section when having geoscientific samples available

. use this section when having video supplements available

## **Appendix A: Figures and tables in appendices**

300 Regarding figures and tables in appendices, the following two options are possible depending on your general handling of figures and tables in the manuscript environment:

### **A1 Option 1**

If you sorted all figures and tables into the sections of the text, please also sort the appendix figures and appendix tables into the respective appendix sections. They will be correctly named automatically.

305 **A2 Option 2**

If you put all figures after the reference list, please insert appendix tables and figures after the normal tables and figures.

To rename them correctly to A1, A2, etc., please add the following commands in front of them: \appendixfigures needs to be added in front of appendix figures \appendixtables needs to be added in front of appendix tables

310 Please add \clearpage between each table and/or figure.

. Contributions

. The authors declare no competing interests.

. We like Copernicus.

. Acknowledgements will go here